JES
JOURNAL OF ENVIRONMENTAL SCIENCES
ISSN 1001-0742
CN 11-2629/X
February 1, 2014 Volume 26 Number 2
www.jesc.ac.cn

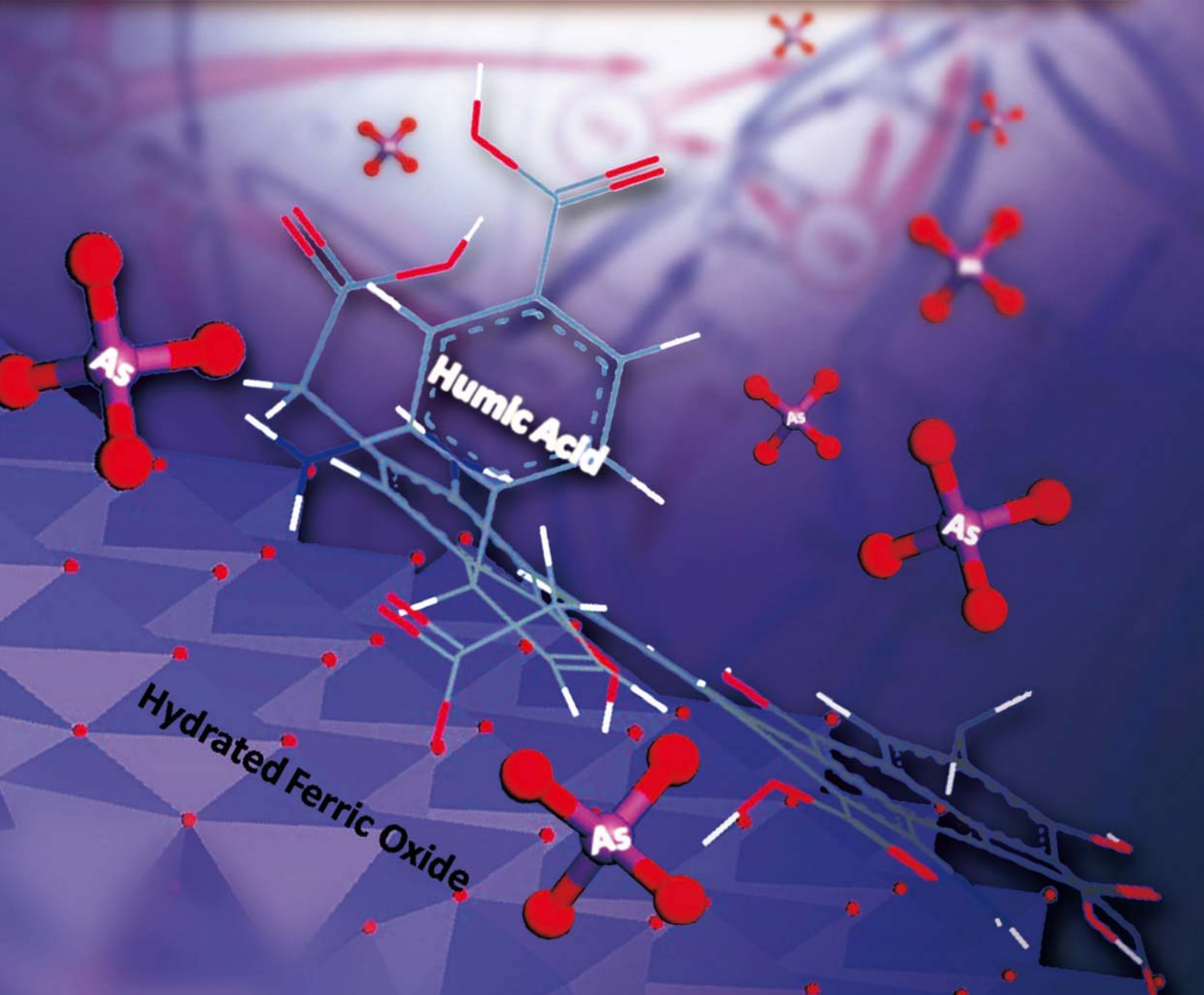


ELSEVIER
Science Press
Sponsored by
Research Center for Eco-Environmental Sciences
Chinese Academy of Sciences

ISSN 1001–0742 **Journal of Environmental Sciences** Vol. 26 No. 2 2014

# CONTENTS

## Aquatic environment



## Atmospheric environment



## Environmental health and toxicology

## Environmental catalysis and materials



Serial parameter: CN 11-2629/X*1989*m*261*en*P*30*2014-2

Journal of Environmental Sciences 26 (2014) 458–465

Available online at www.sciencedirect.com

Journal of Environmental Sciences

www.jesc.ac.cn

# Fabrication of $Bi_2O_3/TiO_2$ nanocomposites and their applications to the degradation of pollutants in air and water under visible-light

Ashok Kumar Chakraborty[1,*], Md Emran Hossain[1], Md Masudur Rhaman[1], K M A Sobahan[2]

*1. Department of Applied Chemistry and Chemical Technology, Islamic University, Kushtia-7003, Bangladesh*

*2. Department of Applied Physics, Electronics and Communication Engineering, Islamic University, Kushtia-7003 Bangladesh*

ARTICLE INFO

Article history:
Received 31 March 2013
revised 19 July 2013
accepted 29 July 2013

*Keywords:*
nanoheterojunction
$Bi_2O_3/TiO_2$ composite
photocatalyst
pollutants
visible-light

DOI: 10.1016/S1001-0742(13)60428-3

ABSTRACT

A nanoheterojunction composite photocatalyst $Bi_2O_3/TiO_2$ working under visible-light ($\lambda \geqslant 420$ nm) was prepared by combining two semiconductors $Bi_2O_3$ and $TiO_2$ varying the $Bi_2O_3/TiO_2$ molar ratio. Maleic acid was employed as an organic binder to unite $Bi_2O_3$ and $TiO_2$ nanoparticles. The SEM, TEM, XRD and diffuse reflectance spectra were utilized to characterize the prepared $Bi_2O_3/TiO_2$ nanoheterojunction. The nanocomposite exhibited unusual high photocatalytic activity in decomposing 2-propanol in gas phase and phenol in aqueous phase and, evolution of $CO_2$ under visible light irradiation while the end members exhibited low photocatalytic activity. The composite was optimized to 5 mol% $Bi_2O_3/TiO_2$. The remarkable high photocatalytic efficiency originates from the unique relative energy band position of $Bi_2O_3$ and $TiO_2$ as well as the absorption of visible light by $Bi_2O_3$.

## Introduction

Photocatalytic degradation of organic pollutants on semiconductor surfaces has attracted much attention as a 'green' technique. $TiO_2$, commonly regarded as one of the most active and stable photocatalysts, has long been investigated for environmental applications (Chen and Mao, 2007; Fujishima et al., 2000; Kubacka et al., 2012). However, the band gap of $TiO_2$ is 3.2 eV which requires the excitation wavelength longer than 387.5 nm. It is a major disadvantage of $TiO_2$ using as a photocatalyst working under visible-light ($\lambda \geqslant 420$ nm). The high rate of electron-hole recombination often results in a low quantum yield and poor efficiency of photocatalytic reactions. Therefore, the development of photocatalysts with a high activity under visible-light irradiation is required. However, an efficient photocatalytic process over a semiconductor demands the high mobility for photoinduced electron–hole separation and for their transportation in crystal lattice, which would lower the probability for electron–hole recombination. Considerable efforts have been made to dope $TiO_2$ with various metals (In et al., 2007; Wang et al., 2000; Song et al., 2012) as well as non-metals so as to make it photoactive under visible light (Anpo and Takeuchi, 2003; Ho et al., 2012; Sato, 1986). Combination of semiconductors is considered as an effective way to improve the photostimulated electron-hole separation and effectively inhibits their recombination. The major characteristic of this technique is to assemble a heterojunction interface between wide and narrow band gap semiconductors with matching energy band potentials. In this way, electric field assisted transportation of charges from one particle to the other through interfaces is favorable for the electron–hole separations in the composite materials, and thus the electron and hole could move to the surface of the semiconductors. The extensive research published on this composite system were mostly focused on $TiO_2$ based pho-

* Corresponding author. E-mail: akc_iu@yahoo.co.uk

tocatalysts, such as $WO_3/TiO_2$, $In_2O_3/TiO_2$, $SiO_2/TiO_2$, $MgO/TiO_2$, $Fe_2O_3/TiO_2$, $Bi_2O_3/TiO_2$, $FeTiO_3/TiO_2$ and so on (Bian et al., 2008; Chakraborty and Kebede, 2012; Ding et al., 2000; Gondal et al., 2004; Gao et al., 2008; Kim et al., 2009; Naeem and Ouyang, 2013; Song et al., 2001).

$Bi_2O_3$, with a band gap of 2.8 eV is known as p-type semiconductor (Hameed et al., 2008; Lin et al., 2007; Xu and Schoonen, 2000), and it has widely been used in gas sensors, optical coatings and solid oxide fuel cells. Moreover, $Bi_2O_3$ has proved to be a good photocatalyst for water splitting and pollutant decomposing under visible-light irradiation (Adamian et al., 1996; Fan et al., 2005; Fruth et al., 2005; Leontie et al., 2002; Yang et al. 2004; Zhou et al., 2009). $Bi_2O_3$ semiconductor possesses good electron ($e^-$) conduction ability. On the other hand, $TiO_2$ has a loosely packed structure as well as higher degree of openness (Lin et al., 2006), which favors the hole ($h^+$) transport in the crystal lattice by the available displacement of the oxygen atoms through the strong vibration model (associated with $O^-$). Thus, in such a heterojunction system, one component, $Bi_2O_3$ of the composite with fair electron ($e^-$) conductivity cooperates with a semiconducting material, $TiO_2$ with an open structure and the fair mobility for the hole ($h^+$) conduction. Hence, when $Bi_2O_3/TiO_2$ heterojunction is formed, the inner electric field will be established in the interface (Lin et al., 2007). The photogenerated electron-hole pairs will be separated effectively by the inner electric field, and the photocatalytic activity is enhanced. Such a phenomenon gives us an implication for a design scheme for the efficient heterojunction photocatalysts between $Bi_2O_3$ and $TiO_2$.

In the present study, we have developed a heterojunction $Bi_2O_3/TiO_2$ system utilizing maleic acid as an organic binder. The role of maleic acid is to bind $Bi_2O_3$ and $TiO_2$ using two end carboxylic functional groups. The prepared $Bi_2O_3/TiO_2$ nanoheterojunction was applied to the photocatalytic degradation of 2-propanol in gas phase and phenol in aqueous phase under visible-light irradiation. The composite $Bi_2O_3/TiO_2$ demonstrated enhanced photocatalytic efficiency compare to that of $Bi_2O_3$ and Degussa P25 under-visible light irradiation.

## 1 Materials and methods

### 1.1 Preparation of $Bi_2O_3/TiO_2$ composite

$Bi_2O_3/TiO_2$ composite photocatalyst was prepared by utilizing maleic acid. Degussa P25 was chosen as the standard $TiO_2$ nanoparticle. In a typical preparation for 5/95 $Bi_2O_3/TiO_2$ (the composite consisting 5 mol% $Bi_2O_3$ and 95 mol% $TiO_2$) heterojunction photocatalyst, 0.3070g of $Bi_2O_3$ (99.9% Aldrich) was suspended in 40 mL of absolute ethanol. A 0.1987 g of maleic acid (99.99% Aldrich) dissolved in absolute ethanol was added to this suspension. Afterward, 1 g of $TiO_2$ nanoparticle was added to the above suspension and stirred vigorously for 6 hr at ambient condition. Subsequently, the suspension was centrifuged and $Bi_2O_3/TiO_2$ composite was washed several times with ethanol to remove unreacted maleic acid. The composite was dried at 60°C in an oven overnight. After that, the $Bi_2O_3/TiO_2$ composite was annealed at 300°C for 3 hr and used as catalyst for photocatalytic degradation reactions without further treatment.

### 1.2 Characterization

The crystallographic phase of prepared samples was characterized by a Rigaku Multiflex diffractometer with monochromated high-intensity Cu $K\alpha$ radiation. XRD scanning was performed under ambient conditions over the $2\theta$ region of 20°–60° at a rate of 2°/min (40 kV, 20 mA). The morphologies of the prepared powders were examined by a scanning electron microscope (Hitachi S-4500). The surface morphology of the $Bi_2O_3/TiO_2$ composite was analyzed by a transmission electron microscope (TEM, Philips CM30) operating at 250 kV. For this measurement, 1 mg of $Bi_2O_3/TiO_2$ composite was dispersed in 50 mL of ethanol, and a drop of the suspension was then spread on a holey amorphous carbon film deposited on a Ni grid (JEOL Ltd.). Diffuse reflectance spectra were also obtained for the dry-pressed disk sample using a UV-Visible spectrometer (Perkin-Elmer Lambda 40).

### 1.3 Measurement of photocatalytic efficiency

The composite $Bi_2O_3/TiO_2$ films were tested as photocatalysts for the decomposition of 2-propanol in gas phase. An aqueous suspension containing $4\times10^{-4}$ mol of $Bi_2O_3/TiO_2$ composite were spread on a 2.5×2.5 Pyrex glass in the film form, which was subsequently dried at 50°C for 2 hr. The gas reactor system used for this photocatalytic reaction is described elsewhere (Kwon et al., 2000). The reaction cell was placed closed to GC and it was connected to GC of which one window is open and the cutoff filter was set in front of this window face of the reaction cell to ensure the desired irradiation condition. The volume of the reaction cell was 200 mL. The film was located at the center of this gastight reactor. After evacuation of the reactor, 0.08 μL of 2-propanol mixed in 1.6 μL of water was injected into the reactor. The total pressure of the reactor was then controlled to 750 Torr by addition of oxygen gas. Under these conditions, 2-propanol and $H_2O$ remained in the vapor phase. The reactor was irradiated from a 300 W Xenon lamp equipped with a water filter and UV filter (< 420 nm, Oriel) to cut off infrared and UV component, respectively. On the surface of the photocatalytic film, the overall light intensity was 0.1 W/cm$^2$. After irradiation for a certain period of time, 0.5 mL of the gas in the reactor was automatically picked up and sent to a gas chromatograph (Agilent Technologies, Model 6890N). The whole photocatalytic reaction was batch process. The

evolved $CO_2$ and remnant 2-propanol were detected by a methanizer installed between the GC column outlet and the FID detector.

The initial concentration of gaseous 2-propanol in the reactor was kept to 117 ppm in volume (ppmV). Thus the ultimate concentration of evolved $CO_2$ will be 351 ppmV when the whole 2-propanol is completely decomposed, as shown in the following Reaction:

$$2(CH_3)_2CHOH(g) + 9O_2(g) \longrightarrow 6CO_2(g) + 8H_2O \quad (1)$$

The photocatalytic activity of the prepared nanocomposite sample was evaluated by the decomposition of phenol in aqueous solution. Each photocatalyst was dispersed in water and then mixed with phenol aqueous solution in darkness. Total volume of the aqueous solution for the photocatalytic reaction was 50 mL, and the concentration of phenol was $1.00\times10^{-4}$ mol/L, and $1.00\times10^{-4}$ mol of photocatalytic sample was suspended in this solution. The prepared solution was then irradiated by a 300-W Xe lamp with an UV cutoff filter (< 420 nm, Oriel) and a water filter to remove IR. The concentration of residual phenol after irradiation was evaluated from the intensity of the characteristic absorption peak.

Prior to photocatalytic reactions, the reaction medium were magnetically stirred for 30 min in the dark, and the concentration of the pollutants were monitored. The concentration of pollutants did not change after stirring for 30 min which indicates that 30 min is enough to reach the adsorption equilibrium of organics. Blank experiments were also performed at the same experimental condition except photocatalyst.

## 2 Results and discussion

In preparing $Bi_2O_3/TiO_2$ heterojunction, maleic acid has been considered. The function of maleic acid is to chemically combine $Bi_2O_3$ and $TiO_2$ nanoparticles utilizing the two carboxylic functional groups as shown in **Scheme 1**.

Thus, the $Bi_2O_3$ and $TiO_2$ nanoparticles move towards each other and, $Bi_2O_3$ and $TiO_2$ could make an intimate contact which is vital for interfacial charge transfer between the two semiconductors. However, the composite was annealed for 300°C to eliminate maleic acid. Hence, the maleic could not influence the photocatalytic activity. The SEM images of pure $Bi_2O_3$ rod and 5/95 $Bi_2O_3/TiO_2$ composite structure are shown in **Fig. 1**. Images in **Fig. 1a, b** reveal the $Bi_2O_3$ exhibits a rod like morphology, where

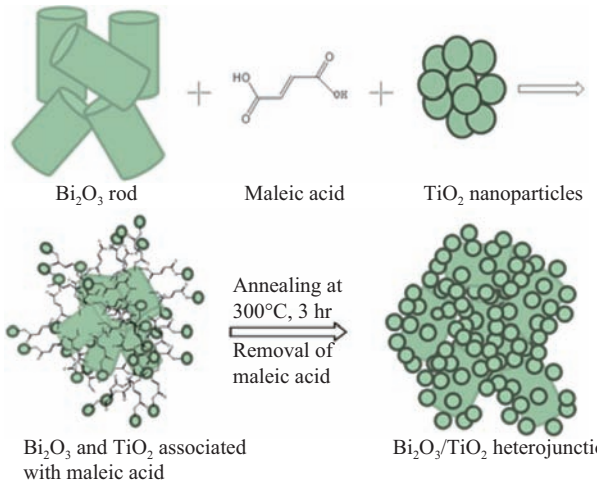


**Scheme 1** Schematic illustration of the formation mechanism of $Bi_2O_3/TiO_2$ heterojunction.

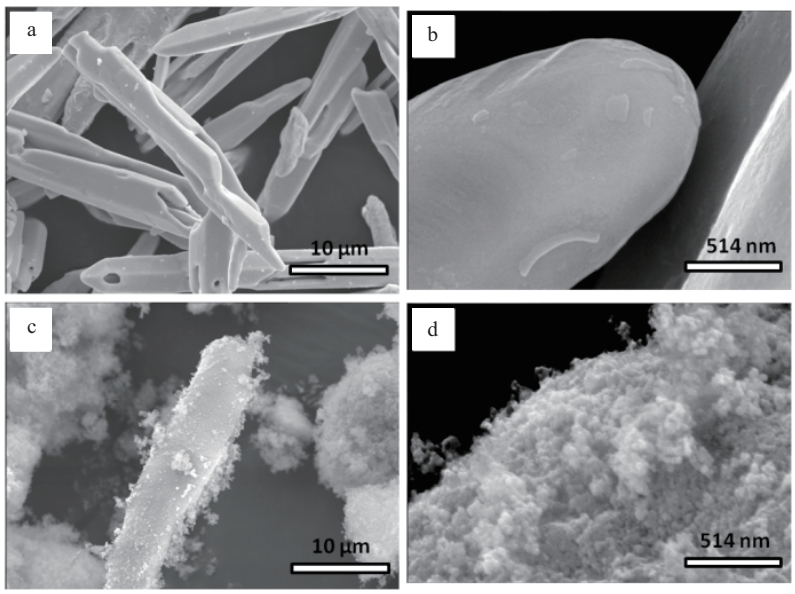


**Fig. 1** SEM images of $Bi_2O_3$ (a, b) and $Bi_2O_3/TiO_2$ (c, d) nanocomposite calcined at 300°C for 3 hr.

the length and diameter of the rods varied over the ranges of 4–33 and 0.4–3.0 μm, respectively. Maleic acid plays a crucial role in combining $Bi_2O_3$ and $TiO_2$ nanoparticles. The surface of $Bi_2O_3$ is fine and smooth as shown in **Fig. 1a, b**. The surface morphology of $Bi_2O_3/TiO_2$ composite is shown in **Fig. 1c, d**. The surface of $Bi_2O_3/TiO_2$ composite is completely different from pure $Bi_2O_3$ and uneven which is shown in **Fig. 1c**. To reveal the detail structure of the composite, **Fig. 1c** was further magnified and shown in **Fig. 1d**. **Figure 1d** clearly demonstrates the surface structure of $Bi_2O_3/TiO_2$ composite that the surface of heterojunction is rough and uniformly covered with $TiO_2$ nanoparticles.

In order to investigate the surface structure and the interface of the composite very closely, the sample of 5/95 $Bi_2O_3/TiO_2$ composite calcined at 300°C was chosen to take TEM and HRTEM characterization. **Figure 2** gives an overview of the typical TEM image of the 5/95 $Bi_2O_3/TiO_2$ composite. Nanoparticles of Degussa P25 with mean size of about 20–30 nm can be observed over the entire surface of $Bi_2O_3$. The high resolution TEM image of the magnified view of the composite is shown in **Fig. 2c, d**. A clear and sharp interface can be found in these images. It is indicated that the two components of the composite are contacted well after the preparation and subsequent heat treatment. The high crystalline quality and the sharp interface between $Bi_2O_3$ and $TiO_2$ nanoparticles are advantageous for the separation of the photogenerated charge carriers.

**Figure 3** shows the XRD patterns of $TiO_2$ nanoparticles, $Bi_2O_3$ and several cmpositions of $Bi_2O_3/TiO_2$ composite samples. The diffraction peaks at 21.82°, 27.48°, 28.12°, 32.61°, 46.49°, 52.56° and 54.99° were indexed to the (020), (120), (012), (211), (223), (321) and (241) planes, respectively to the pure $Bi_2O_3$ (JCPDS #72-0398). As shown in **Fig. 3** that the diffraction planes of (101), (004), (200) and (211) clearly indicate the presence of anatase and that of (110) and (101) planes demonstrate the existence of rutile phase of $TiO_2$ nanopartiles. Hence, Degussa P25 contains anatase and rutile phase. It is worth mentioning that the XRD patterns of the composites $Bi_2O_3/TiO_2$ showed the diffraction peaks of phases of $Bi_2O_3$ and $TiO_2$ without any other impurity phases suggesting that there was no sufficient chemical reaction took place among the component $Bi_2O_3$ and $TiO_2$ of the composite during the preparation of heterojunction and subsequent heat-

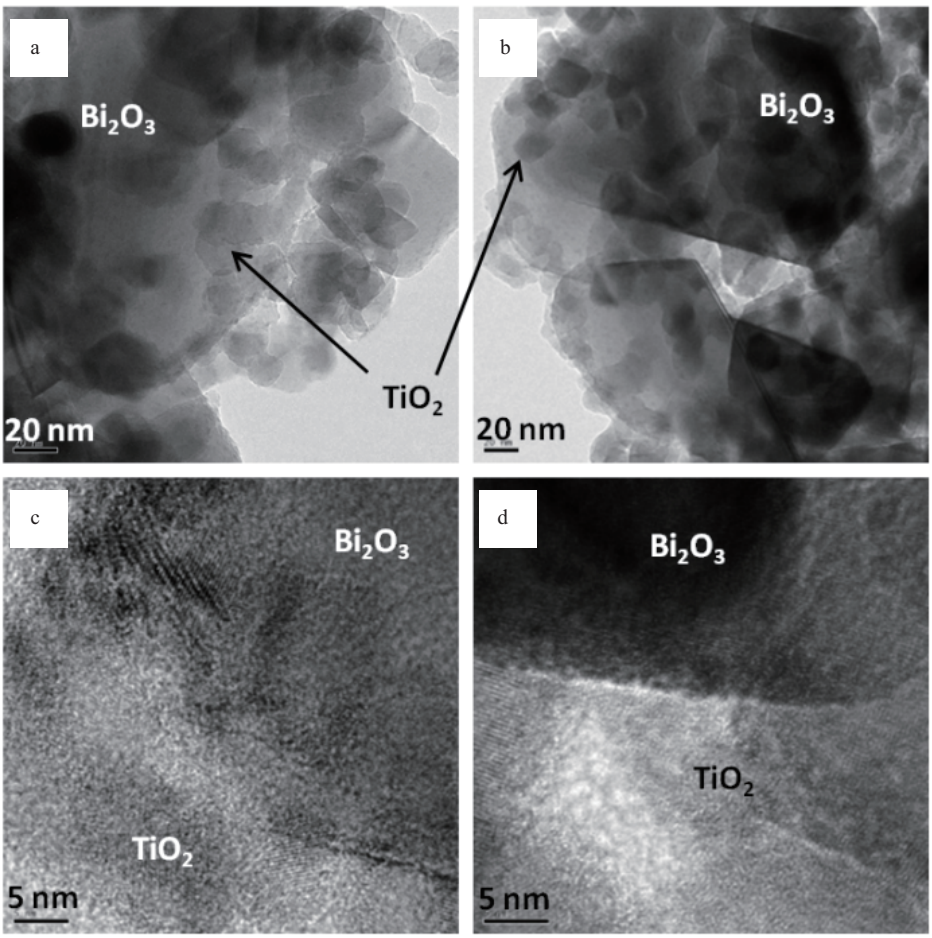


**Fig. 2** TEM (a, b) and HRTEM (b, c) images of 5/95 $Bi_2O_3/TiO_2$ heterojunction calcined at 300°C for 3 hr.

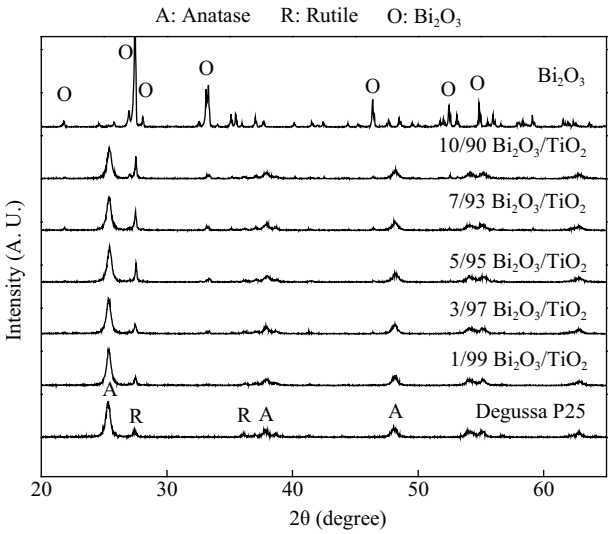


**Fig. 3** X-ray diffraction pattern of $TiO_2$, $Bi_2O_3$ and $Bi_2O_3/TiO_2$ composite synthesized at 300°C for 3 hr with several composition of $Bi_2O_3$ and $TiO_2$.

treatment at 300°C. As shown in **Fig. 3** that the intensity of the major peak of $Bi_2O_3$ of (120) plane at 27.48° gradually increases with increasing amount of $Bi_2O_3$ from 0% to 100% in the composite $Bi_2O_3/TiO_2$. However, the annealing temperature 300°C is sufficiently enough to make a tight contact between $Bi_2O_3$ and $TiO_2$ nanoparticles as shown in **Fig. 2c** and **d**. The well contact will facilitate interparticle electron transfer between $Bi_2O_3$ and $TiO_2$.

The UV-Vis diffuse reflectance spectra of the as-prepared composite powders are shown in **Fig. 4.** The band gaps of $Bi_2O_3$ and $TiO_2$ were reported to be 2.8 and 3.2 eV, respectively (Hameed et al., 2008; Xu and Schoonen, 2000). The optical absorptions of $Bi_2O_3/TiO_2$ composite powders start at about 450 nm, corresponding to the absorption edge of $Bi_2O_3$. The second absorption edge at about 387 nm can be attributed to the $TiO_2$ nanoparticles. It is mentionable from **Fig. 4** that with increasing the

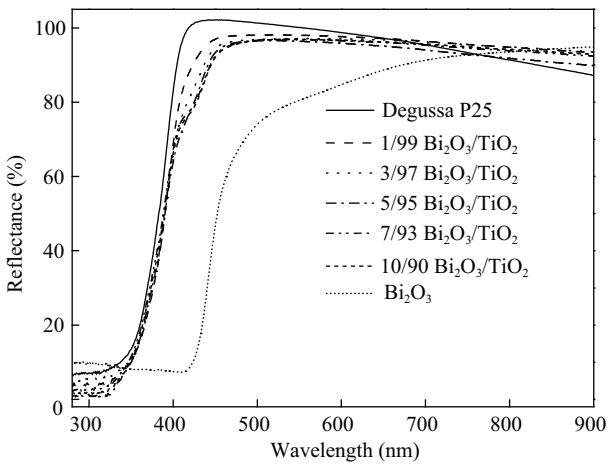


**Fig. 4** UV-Visible diffuse reflectance spectra of $Bi_2O_3/TiO_2$ composite, $Bi_2O_3$ and $TiO_2$ nanoparticle.

component of the $Bi_2O_3$ in the composite $Bi_2O_3/TiO_2$ system, the absorption in visible-light of the composite powders also increased. These results revealed that the composite powders could absorb the photon in the visible region of the solar spectrum.

The dependence of photocatalytic activity on the composition of the composite $Bi_2O_3/TiO_2$ system under visible light ($\lambda \geqslant 420$ nm) irradiation is represented in **Fig. 5**. The catalyst samples were evaluated for the degradation of 2-propanol and the production of $CO_2$ in gas phase and phenol in aqueous phase under visible light irradiation at room temperature. It is generally accepted that IP is first decomposed to acetone and finally to $CO_2$. Thus, we measured the photocatalytic decomposition behavior of IP first. **Figure 5a** shows the visible light ($\lambda \geqslant 420$ nm) activity of the

$Bi_2O_3$, $TiO_2$ and $Bi_2O_3/TiO_2$ composite photocatalyst for the decomposition of 2-propanol. $Bi_2O_3$, $TiO_2$ exhibited negligible activity, while $Bi_2O_3/TiO_2$ in several compositions showed higher visible light induced photocatalytic activity. When photocatalytic reaction proceeded for 2 hr, the decomposition degrees of gaseous 2-propanol was 75% with 5/95 $Bi_2O_3/TiO_2$ heterojunction as shown in **Fig. 5a**.

The photocatalytic efficiency of the composite sample was investigated for the evolution of $CO_2$. **Figure 5b** displays the photocatalytic behavior of $Bi_2O_3/TiO_2$ composite samples including the component of the composite $Bi_2O_3$ and Degussa P25 to compare the efficiency. The composite $Bi_2O_3/TiO_2$ samples with a wide range of composition demonstrated significant production of $CO_2$. As that of the decomposition of gaseous 2-propanol, 5/95 $Bi_2O_3/TiO_2$ demonstrated the highest activity among the composition for the production $CO_2$. After 2 hr of visible light ($\lambda \geqslant 420$ nm) irradiation, the detected $CO_2$ yield was reached to a stable value of 21 ppmV, whereas both the bare $Bi_2O_3$ and Degussa P25 showed only 2.1 and 2.9 ppmV, respectively.

We evaluated the photocatalytic activities of these catalysts in aqueous phase for the decomposition of phenol under visible light ($\lambda \geqslant 420$ nm). The remnant phenol after the irradiation of visible light was analyzed from its characteristic absorption peak detected by UV–vis spectroscopy. **Figure 5c** shows decomposition rates of phenol with several $Bi_2O_3/TiO_2$ composition, $Bi_2O_3$, and P25 samples as a function of irradiation time. It was found that the photocatalytic activity of the composite was increased with increasing $Bi_2O_3$. Similar results were obtained as that of decomposition of gaseous 2-propanol, 5/95 $Bi_2O_3/TiO_2$ showed the highest photocatalytic efficiency in decomposing phenol in aqueous phase. The decomposition of phenol was 69% with this composition in 2 hr of visible light irradiation. Blank experiments as shown in **Fig. 5** that the photodecomposition of the organics in gas and aqueous phases was not took place.

Coupling of $TiO_2$ with other narrow band gap semi-

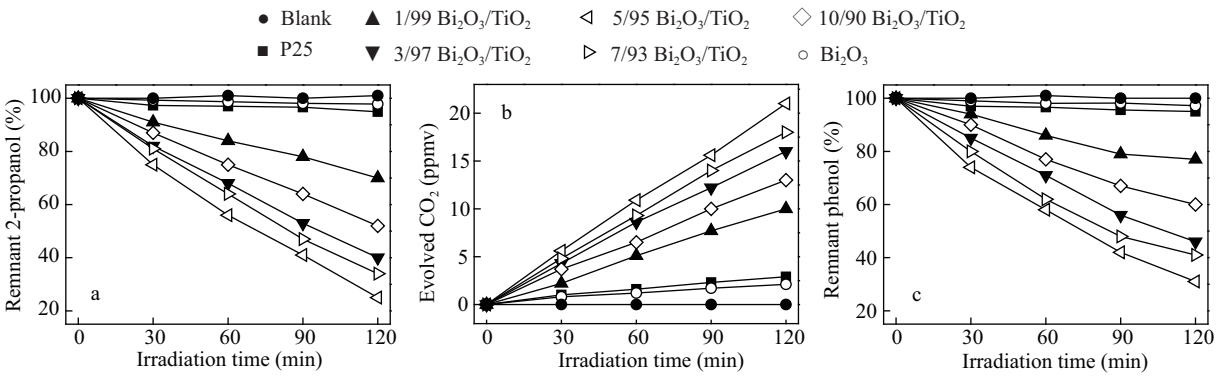


**Fig. 5** Photocatalytic activity of $TiO_2$, $Bi_2O_3$ and $Bi_2O_3/TiO_2$ composite for (a) degradation of 2-propanol, (b) evolution of $CO_2$ and (c) decomposition of phenol under visible light ($\lambda \geqslant 420$ nm) irradiation.

conductors has been extensively studied to promote the separation of photogenerated charge-carriers and/or to extend the absorption of photon up to visible-region as well as to enhance the photocatalytic behavior in decomposing organic pollutants. The present investigated heterojunction $Bi_2O_3/TiO_2$ exhibited extraordinary high photocatalytic efficiency but both the components $Bi_2O_3$ and $TiO_2$ demonstrated very low photocatalytic activity under visible-light irradiation. Presumably, the unusual high photocatalytic activity of $Bi_2O_3/TiO_2$ originates from the unique relative energy band positions of these two semiconductors (Chai et al., 2009; Chakraborty and Kebede, 2012; Chakraborty et al., 2012; Gao et al., 2008, 2010; Kim et al., 2009) and the absorption of visible light by $Bi_2O_3$. As shown in **Fig. 6**, the VB of $Bi_2O_3$ is located below than that of $TiO_2$ by 0.22V, while CB of $Bi_2O_3$ is positioned below than that of the $TiO_2$ by 0.62V (Hameed et al., 2008; Xu and Schoonen, 2000). During visible-light irradiation, $Bi_2O_3$ absorbs visible-light as the band gap of $Bi_2O_3$ is 2.8 eV and the electrons ($e^-$) in the VB of $Bi_2O_3$ would be excited to its CB and the VB of $Bi_2O_3$ become partially vacant, and the generated holes ($h^+$) in the VB of $Bi_2O_3$ can be transferred to VB of $TiO_2$, since the VB of $TiO_2$ is located higher than the VB of $Bi_2O_3$. Thus, the holes ($h^+$) in the VB of $TiO_2$ can be utilized for various oxidation reactions.

The CB potential of $Bi_2O_3$ is +0.33V. Hence, the reduction of oxygen utilizing single electron is quite difficult (Reactions (2) and (3)). Thus, the CB electrons of $Bi_2O_3$ would be consumed through multi-electron process (Abe et al., 2008; Liu et al., 2009; Rawal et al., 2012) according to following reactions (Reactions (4) and (5)).

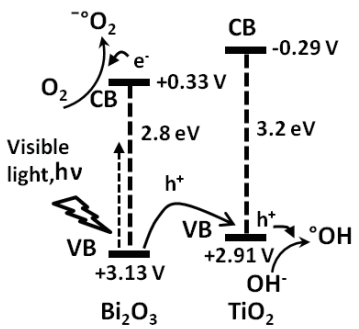


**Fig. 6** Proposed mechanism for the photocatalytic degradation of organic pollutants over $Bi_2O_3/TiO_2$ heterojunction photocatalyst.

$$O_2 + e^- = O_2^-; \quad E^0 = -0.284 \text{ V (vs. NHE)} \quad (2)$$

$$O_2 + H^+ + e^- = HO_2; \quad E^0 = -0.046 \text{ V (vs. NHE)} \quad (3)$$

$$O_2 + 2H^+ + 2e^- = H_2O_2; \quad E^0 = +0.682 \text{ V (vs. NHE)} \quad (4)$$

$$O_2 + 4H^+ + 4e^- = 2H_2O; \quad E^0 = +1.23 \text{ V (vs. NHE)} \quad (5)$$

By the inter-semiconductor hole-transfer mechanism, the photogenerated charge-carriers can be effectively separated so that this heterojunction can utilize the visible-light in mineralizing organic pollutants. In this photocatalytic system, $TiO_2$ works as principal photocatalyst, while the role of $Bi_2O_3$ is a sensitizer absorbing visible-light to sensitize $TiO_2$. We expect that this synthesis process can also be extended to the development of other heterojunction type composite photocatalysts working under sunlight to remove organic pollutants.

## 3 Conclusions

A series of $Bi_2O_3/TiO_2$ heterocomposite photocatalyst have been prepared by utilizing maleic acid. It was observed that the composite could absorb energy up to visible-region. The new composite demonstrated notably higher photocatalytic activity for the degradation of 2-propanol in gas phase and phenol in aqueous phase and, evolution of $CO_2$ than $Bi_2O_3$ and $TiO_2$ nanoparticles under visible light ($\lambda \geqslant 420$ nm) irradiation. After 2 hr of visible light ($\lambda \geqslant 420$ nm) irradiation, the decomposition of 2-propanol and phenol is 75% and 69%, respectively and, the evolution of $CO_2$ is 21 ppmV. The evolved $CO_2$ is about 7.5 times that of Degussa P25. $TiO_2$ works as a principal photocatalyst while $Bi_2O_3$ acts as the photosensitizer absorbing visible light in the $Bi_2O_3/TiO_2$ composite.

The extraordinary high photocatalytic efficiency of the $Bi_2O_3/TiO_2$ composite originates from the unique relative energy band position of the component semiconductors. The VB level of $Bi_2O_3$ (+3.13V vs. NHE) is located lower than that of $TiO_2$ (+2.91V vs. NHE). The visible light generated hole ($h^+$) in the VB of $Bi_2O_3$ can be transferred to the VB of $TiO_2$. Therefore, with the irradiation of visible light the holes ($h^+$) in the VB of $TiO_2$ can induce the complete decomposition of organic pollutants.

## Acknowledgments

The authors gratefully acknowledge the Evonik Degussa GmbH for Degussa P25.

## REFERENCES

Abe, R., Takami, H., Murakami, N., Ohtani, B., 2008. Pristine simple oxides as visible light driven photocatalysts: Highly efficient decomposition of organic compounds over platinum-loaded tungsten oxide. J. Amer. Chem. Soc. 130, 7780–7781.

Bian, Z. F., Zhu, J., Wang, S. H., Cao, Y., Qian, X. F., Li, H. X., 2008. Self-assembly of active $Bi_2O_3/TiO_2$ visible photocatalyst with ordered mesoporous structure and highly crystallized anatase. J. Phys. Chem. 112, 6258–6262.

Chai, S. Y., Kim, Y. J., Jung, M. H., Chakraborty, A. K., Jung, D. W., Lee, W. I., 2009. Heterojunctioned $BiOCl/Bi_2O_3$, A new visible light photocatalyst. J. Catal. 262, 144–149.

Chakraborty, A. K., Kebede, M. A., 2012a. Preparation and characterization of $WO_3/Bi_3O_4Cl$ nanocomposite and its photocatalytic behavior under visible light irradiation. Reaction Kinetics, Mechani. Catal. 106, 83–98.

Chakraborty, A. K., Ganguli, S., Kebede, M. A., 2012. Photocatalytic degradation of 2-propanol and phenol using Au loaded $MnWO_4$ nanorod under visible light irradiation. J. Cluster Sci. 23, 437–448.

Chakraborty, A. K., Kebede, M. A., 2012b. Efficient decomposition of organic pollutants over $In_2O_3/TiO_2$ nanocomposite photocatalyst under visible light irradiation. J. Cluster Sci. 23, 247–257.

Ding, Z., Hu, X., Lu, G. Q., Yue, P. L., Greenfield, P. F., 2000. Novel silica gel supported $TiO_2$ photocatalyst synthesized by CVD method. Langmuir 16, 6216–6222.

Fan, H. T., Teng, X. M., Pan, S. S., Ye, C., Li, G. H., Zhang, L. D., 2005. Optical properties of $\delta$-$Bi_2O_3$ thin films grown by reactive sputtering. Appl. Phys. Lett. 87, 231916–231918.

Fruth, V., Popa, M., Berger, D., Ramer, R., Gartner, M., Ciulei, A. et al., 2005. Deposition and characterisation of bismuth oxide thin films. J. Eur. Ceram. Soc. 25, 2171–2174.

Fujishima, A., Rao, T. N., Tryk, D. A., 2000. Titanium dioxide photocatalysis. J. Photochem. Photobiol. C 1, 1–21.

Gao, B. F., Kim, Y. J., Chakraborty, A. K., Lee, W. I., 2008. Efficient decomposition of organic compounds with $FetiO_3/TiO_2$ heterojunction under visible light irradiation. Appl. Catal. B: Environ. 83, 202–207.

Gao, B. F., Chakraborty, A. K., Yang, J. M., Lee, W. I., 2010. Visible-light photocatalytic activity of $BiOCl/Bi_3O_4Cl$ nanocomposites. Bull. Korean Chem. Soc. 31, 1941–1944.

Gondal, M. A., Hameed, A., Yamani, Z. H., Suwaiyan, A., 2004. Laser induced photo-catalytic oxidation/splitting of water over $\alpha$-$Fe_2O_3$, $WO_3$, $TiO_2$ and NiO catalysts: Activity comparison. Chem. Phys. Lett. 385, 111–115.

Hameed, A., Montini, T., Gombac, V., Fornasiero, P., 2008. Surface phases and photocatalytic activity correlation of $Bi_2O_3/Bi_2O_4$-x nanocomposite. J. Amer. Chem. Soc. 130, 9658–9659.

In, S., Orlov, A., Berg, R., Garcia, F., Jimenez, S. P., Tikhov, M. S. et al., 2007. Effective visible light-activated B-doped and B, N-codoped $TiO_2$ photocatalysts. J. Amer. Chem. Soc. 129, 13790–13791.

Kim, Y. J., Gao, B., Han, S. Y., Jung, M. H., Chakraborty, A. K., Ko, T. et al., 2009. Heterojunction of $FetiO_3$ nanodisc and $TiO_2$ nanoparticle for a novel visible light photocatalyst. J. Phys. Chem. C 113, 19179–19184.

Kubacka, A., Fernández-García, M., Colón, G., 2012. Advanced nanoarchitectures for solar photocatalytic applications. Chem. Rev. 112, 1555–1614.

Kwon, Y. T., Song, K. Y., Lee, W. I., Choi, G. J., Do, Y. R., 2000. Photocatalytic behavior of $WO_3$-loaded $TiO_2$ in an oxidation reaction. J. Catal. 191, 192–199.

Leontie, L., Caraman, M., Alexe, M., Harnagea, C., 2002. Structural and optical characteristics of bismuth oxide thin films. Surf. Sci. 507-510, 480–485.

Lin, X. P., Xing, J. C., Wang, W. D., Shan, Z. C., Xu, F. F., Huang, F. Q., 2007. Photocatalytic activities of heterojunction semiconductors $Bi_2O_3/BaTiO_3$: A strategy for the design of efficient combined photocatalysts. J. Phys. Chem. C 111, 18288–18293.

Lin, X. P., Huang, F. Q., Wang, W. D., Wang, Y. M., Xia, Y. J., Shi, L. L., 2006. Photocatalytic activities of $M_2Sb_2O_7$ (M = Ca, Sr) for degrading methyl orange. Appl. Catal. 313, 218–223.

Liu, G., Wang, L. Z., Sun, C. H., Yan, X. X., Wang, X. W., Chen, Z. G. et al., 2009. Band-to-band visible-light photon excitation and photoactivity induced by homogeneous nitrogen doping in layered titanates. Chem. Mater. 21, 1266–1274.

Naeem, K., Ouyang, F., 2013. Influence of supports on photocatalytic degradation of phenol and 4-chlorophenol in aqueous suspensions of titanium dioxide. J. Environ. Sci. 25, 399–404.

Rawal, S. B., Chakraborty, A. K., Kim, Y. J., Kim, H. J., Lee, W. I., 2012. Double-heterojunction structure of $SbxSn1\text{-}xO_2/TiO_2/CdSe$ for efficient decomposition of gaseous 2-propanol under visible-light irradiation. RSC Advances 2, 622–630.

Song, K. Y., Park, M. K., Kwon, Y. T., Lee, H. W., Chung, W. J., Lee, W. I., 2001. Preparation of transparent particulate $MoO_3/TiO_2$ and $WO_3/TiO_2$ films and their photocatalytic properties. Chem. Mater. 13, 2349–2355.

Wang, C., Bahnemann, D. W., Dohrmann, J. K., 2000. A novel preparation of iron-doped $TiO_2$ nanoparticles with enhanced photocatalytic activity. Chem. Commun. 16, 1539–1540.

Xu, Y., Schoonen, M. A. A., 2000. The absolute energy positions of conduction and valence bands of selected semiconducting minerals. Amer. Miner. 85, 543–556.

Yang, B. J., Mo, M. S., Hu, H. M., Li, C., Yang, X. G., Li, Q. et al., 2004. A Rational self-sacrificing template route to $\beta$-$Bi_2O_3$ nanotube arrays. Eur. J. Inorg. Chem. 2004, 1785–1787.

Song, S. Z., Sheng, Z. Y., Liu, Y., Wang, H. Q., Wu, Z. B., 2012. Influences of pH value in deposition-precipitation synthesis process on Pt-doped $TiO_2$ catalysts for photocatalytic oxidation of NO. J. Environ. Sci. 24, 1519–1524.

Sato, S., 1986. Photocatalytic activity of NOx-doped $TiO_2$ in the visible light region. Chem. Phys. Lett. 123, 126–128.

Adamian, Z. N., Abovian, H. V., Aroutiounian, V. M., 1996. Smoke sensor on the base of $Bi_2O_3$ sesquioxide. Sens. Actuat. B: Chem. 35, 241–243.

Anpo, M., Takeuchi, M., 2003. The design and development of highly reactive titanium oxide photocatalysts operating under visible light irradiation. J. Catal. 216, 505–516.

Chen, X. B., Mao, S. S., 2007. Titanium dioxide nanomaterials: Synthesis, properties, modifications, and applications. Chem. Rev. 107, 2891–2959.

Zhou, L., Wang, W. Z., Xu, H. L., Sun, S. M., Shang, M., 2009. $Bi_2O_3$ Hierarchical nanostructures: Controllable synthesis, growth mechanism, and their application in photocatalysis. Chem. A Eur. J. 15, 1776–1782.

Ho, L. N., Ong, S. A., Osman, H., Chong, F. M., 2012. Enhanced photocatalytic activity of fish scale loaded $TiO_2$ composites under solar light irradiation. J. Environ. Sci. 24, 1142–1148.

# Editorial Board of Journal of Environmental Sciences

# JOURNAL OF ENVIRONMENTAL SCIENCES

环境科学学报(英文版)

**(http://www.jesc.ac.cn)**

**Aims and scope**

*Journal of Environmental Sciences* is an international academic journal supervised by Research Center for Eco-Environmental Sciences, Chinese Academy of Sciences. The journal publishes original, peer-reviewed innovative research and valuable findings in environmental sciences. The types of articles published are research article, critical review, rapid communications, and special issues.

The scope of the journal embraces the treatment processes for natural groundwater, municipal, agricultural and industrial water and wastewaters; physical and chemical methods for limitation of pollutants emission into the atmospheric environment; chemical and biological and phytoremediation of contaminated soil; fate and transport of pollutants in environments; toxicological effects of terrorist chemical release on the natural environment and human health; development of environmental catalysts and materials.

**For subscription to electronic edition**

Elsevier is responsible for subscription of the journal. Please subscribe to the journal via http://www.elsevier.com/locate/jes.

**For subscription to print edition**

China: Please contact the customer service, Science Press, 16 Donghuangchenggen North Street, Beijing 100717, China. Tel: +86-10-64017032; E-mail: journal@mail.sciencep.com, or the local post office throughout China (domestic postcode: 2-580).

Outside China: Please order the journal from the Elsevier Customer Service Department at the Regional Sales Office nearest you.

**Submission declaration**

Submission of an article implies that the work described has not been published previously (except in the form of an abstract or as part of a published lecture or academic thesis), that it is not under consideration for publication elsewhere. The submission should be approved by all authors and tacitly or explicitly by the responsible authorities where the work was carried out. If the manuscript accepted, it will not be published elsewhere in the same form, in English or in any other language, including electronically without the written consent of the copyright-holder.

**Submission declaration**

Submission of the work described has not been published previously (except in the form of an abstract or as part of a published lecture or academic thesis), that it is not under consideration for publication elsewhere. The publication should be approved by all authors and tacitly or explicitly by the responsible authorities where the work was carried out. If the manuscript accepted, it will not be published elsewhere in the same form, in English or in any other language, including electronically without the written consent of the copyright-holder.

**Editorial**

Authors should submit manuscript online at http://www.jesc.ac.cn. In case of queries, please contact editorial office, Tel: +86-10-62920553, E-mail: jesc@263.net, jesc@rcees.ac.cn. Instruction to authors is available at http://www.jesc.ac.cn.


**Journal of Environmental Sciences (Established in 1989)**

**Vol. 26 No. 2 2014**

| | | | |
|---|---|---|---|
| **Supervised by** | Chinese Academy of Sciences | **Published by** | Science Press, Beijing, China |
| **Sponsored by** | Research Center for Eco-Environmental | | Elsevier Limited, The Netherlands |
| | Sciences, Chinese Academy of Sciences | **Distributed by** | |
| **Edited by** | Editorial Office of Journal of | Domestic | Science Press, 16 Donghuangchenggen |
| | Environmental Sciences | | North Street, Beijing 100717, China |
| | P. O. Box 2871, Beijing 100085, China | | Local Post Offices through China |
| | Tel: 86-10-62920553; http://www.jesc.ac.cn | Foreign | Elsevier Limited |
| | E-mail: jesc@263.net, jesc@rcees.ac.cn | | http://www.elsevier.com/locate/jes |
| **Editor-in-chief** | Hongxiao Tang | **Printed by** | Beijing Beilin Printing House, 100083, China |

**CN 11-2629/X** **Domestic postcode: 2-580** **Domestic price per issue RMB ¥ 110.00**

ISSN 1001-0742